Supporting Information:

Inducing nano-confined crystallization in semicrystalline polymers by elastic melt stretching

Masoud Razavi[1], Wenwen Zhang[2], Liangbin Li[2]*, Hossein Ali Khonakdar[3,4], Andreas Janke[3] and Shi-Qing Wang[1]*

[1]College of Polymer Science and Engineering, University of Akron, Akron, OH
[2]National Radiation Laboratory, University of Science and Technology of China, Hefei, China
[3]Leibniz Institute of Polymer Research, D-01067 Dresden, Germany
[4]Iran Polymer and Petrochemical Institute, P.O. Box 14965/115, Tehran, Iran

A. Materials:

Two commercial semi-crystalline polymers, poly(l-lactic acid) (PLLA) and poly(ethylene terephthalate) (PET) were used in this study. The weight average molecular weight M_w, entanglement molecular weight M_e and glass transition T_g of these polymers are listed in Table S.1.

Table S.1. Molecular characteristics of studied semi-crystalline polymers

Polymer	Mw (kg/mol)	M_e (kg/mol)	T_g (°C)	T_m (°C)	Source
PLLA	115	3.24	60	175	Nature Works (Ingeo 3100HP)
PET	-	1.45	80	250	Eastman (7352 PET)

B. Sample preparation:

In order to remove moisture from PLLA, the resins were initially dried in temperature-controlled chamber (Thelco GCA Precision, model 18) for several hours. For the uniaxial tensile tests and melt-stretching, dog-bone samples were made from compression molding of the resins using a Carver Press. The sample dimensions are length by width by thickness equal to $39 \times 3 \times 0.6$ mm^3. The applied load during molding was equal to 9000 kg. PLLA and PET resins were first heated above their respective melting points of 210 °C and 290 °C and then, after minutes, were quickly quenched into icy water to obtain amorphous PLLA and PET. To obtain cold-crystallized isotropic samples, the amorphous PLLA and PET samples were annealed in the temperature-controlled chamber respectively at 90-100 °C and 150-160 °C for 4 hours. The subsequent Section C.2 describes the production of the pre-melt-stretched PLLA and PET samples.

C. Experimental procedures:

C.1. Mechanical tests:

[1] Corresponding authors: lbl@ucst.edu.cn, swang@uakron.edu

Uniaxial tensile tests of either dog-bone shaped or stripe like samples (cut from the middle part of melt-stretched samples), were carried out using Instron 5969, equipped with a temperature-controlled chamber. The temperature controller for Instron has an accuracy of ±1 °C. Uniaxial extensional tests were conducted with various constant cross-head speeds V, corresponding to an initial drawing rate V/L_0, where L_0 is the initial specimen length. Drawing rate V/L_0 for the mechanical measurements, presented in Fig. 6 and Fig. S.3, was set equal to 0.5 min^{-1}.

C.2. Melt stretching:

Instron 5969 was used to perform melt stretching and step-strain tests. For these experiments, the Instron was programed using Bluehill software to apply a constant Hencky rate $\dot{\varepsilon}$, i.e. keeping constant V/L where the L is instantaneous length during stretching. Two types of dog-bone shape samples with the sizes of 10 × 1.5 × 3 mm^3 and 35 × 2 × 8 mm^3 (length × thickness × width) were used. Melt-stretching of amorphous PLLA and PET was carried out at Hencky rate $\dot{\varepsilon}$= V/L = 0.027 s^{-1} and T = 70 ˚C and 0.054 s^{-1} and 85 ˚C respectively. For PLLA, this corresponds to *Wi* = 118, where the Weissenberg number *Wi* is a product of (V/L) and the terminal relaxation time τ = 4380 s [1]. Figs. S.1(a-c) indicate the melt stretching behavior of these samples. In the case of PLLA it was found that after physical aging the onset of upturn in the mechanical stress data, indicative of strain-induced crystallization takes place at a lower stretching ratio, as shown in Fig. S.1(b). The effect of aging on quiescent crystallization has been noted before [2]. Thus, the observed effect is perhaps unsurprising. The cold-crystallization from annealing of pre-melt-stretched PLLA, presented in Fig. 2 and Fig. 5, involved freshly prepared, non-aged PLLA. In contrast, the *in situ* WAXD measurements in Fig. 4 was based on an aged PLLA. For PLLA, physical aging readily occurs during storage at room temperature for several hours. The effect of melt-stretching was preserved by immediate thermal quenching to room temperature by spraying icy water onto the specimen at the end of the melt-stretching.

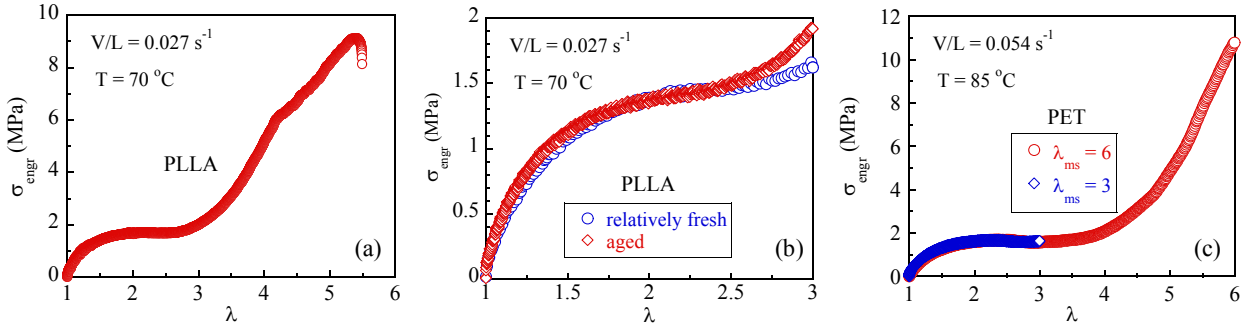

Fig. S.1. Engineering stress σ_{engr} vs stretching ratio $\lambda = L/L_0$ during melt-stretching of (a) freshly-prepared amorphous PLLA until it fails at a high stretching ratio (b) freshly prepared and aged amorphous PLLA until $\lambda_{ms} = 3$ and (c) amorphous PET to λ_{ms} of 3 and 6.

C.3. Custom-built annealing device (heater):

A custom-built heater [3] was employed to achieve quick annealing of pre-melt-stretched amorphous PLLA and PET. The procedure is as follows. First, a specimen is mounted onto the

Instron at room temperature. Before annealing the Instron reads zero tensile stress. The heater is made of two hot metal plates with a narrow gap and is preset to a given temperature, e.g., 70 ˚C for PLLA and 100 ˚C for PET. To start the annealing test, we first began to record the stress using Instron which read zero. Then the specimen was brought into the hot narrow gap. Fig. 2(b) represents the stress data during annealing of a pre-melt-stretched PLLA and shows that the heater was introduced to heat up the specimen at t = ca. 20 s. In contrast, the oven used to heat up the samples for *in situ* x ray scattering measurements takes nearly three hundred seconds to reach 70 ^{o}C from room temperature as indicated in Fig. 5.

C.4. Atomic force microscope measurements:

The samples were microtomed in the direction parallel to the stretching direction to generate a smooth surface. The measurements were done in a non-calibrated PF-QNM mode (peak force tapping - quantitative nanomechanical mapping) using a Dimension Icon (Bruker-Nano, USA) equipped with a heating stage. ScanAsyst fluid + cantilever (Bruker-Nano) with a nominal spring constant of 0.7 N/m and a nominal tip radius of 2 nm were used. The image modification and analysis was done by NanoScope Analysis (Bruker-Nano).

C.5. Scattering studies:

Ex situ (after crystallization and stretching) x-ray scattering measurements were preformed using lab-scale wide-angle x-ray scattering (WAXD) apparatus or synchrotron radiation in both modes of WAXD and small-angle (SAXS). Real-time WAXD and SAXS measurements along with temperature and/or stress during annealing or stretching, were carried out using the *in situ* synchrotron radiation. Besides the information presented in Figures 4 and 5, our *in situ* measurements also examined the crystallization process during melt stretching. Such results are omitted here. The details of the x-ray sources are as follows:

Lab-scale WAXD apparatus: rotating anode X-ray generator (RU 300, 12 kW, Rigaku, Woodlands, TX), which produces a beam of ponochromatic Cu Kα radiation (λ = 1.54 Å). For this device the X-ray generator operates at 40 kV 134 and 30 mA.

WAXD and SAXS synchrotron radiation were carried out in BL19U (λ = 1.03 Å) beamline in the Shanghai Synchrotron Radiation Facility (SSRF). Pilatus 200K and Pilatus 1M detector was used to collect 2D WAXD and SAXS patterns respectively with 0.1s and 5s exposure time. The corresponding sample-to detector distances calibrated for WAXD and SAXS were 74 and 2100 mm, respectively. A homemade apparatus was used in this work, which was equipped with a hot air blower to achieve a uniform heating environment of the sample with the accuracy of roughly ±0.5 ^{o}C. Two temperature probes were set in the heating/stretching chamber to realize the real-time detection of the temperature of the environment where the sample is located.

C.6. Further information:

The super strong mechanical properties of PLLA arise from the geometric condensation [4] of the chain network due to the pre-melt stretching. The same effect of melt stretching is responsible [5]

for turning brittle polystyrene ductile at room temperature [6, 7]. It is also worth noting that in absence of the pre-melt stretching, crystalline PLLA is complete brittle [8], regardless of whether it was obtained either from annealing of amorphous PLLA to attain cold crystallization or from isothermal (ca. 110-120 °C) melt crystallization. These crystalline PLLA are opaque since the sizes of spherulites range from microns to hundreds of microns.

D. Additional Data:

D.1. Differential Scanning Calorimetry (DSC) of PLLA and PET:

Fig. S.4a and b show the DSC curve of pure PLLA and PET recorded in a cycle of heating-cooling-heating, Values of melting and crystallization temperature were read from 2nd heating and first cooling.

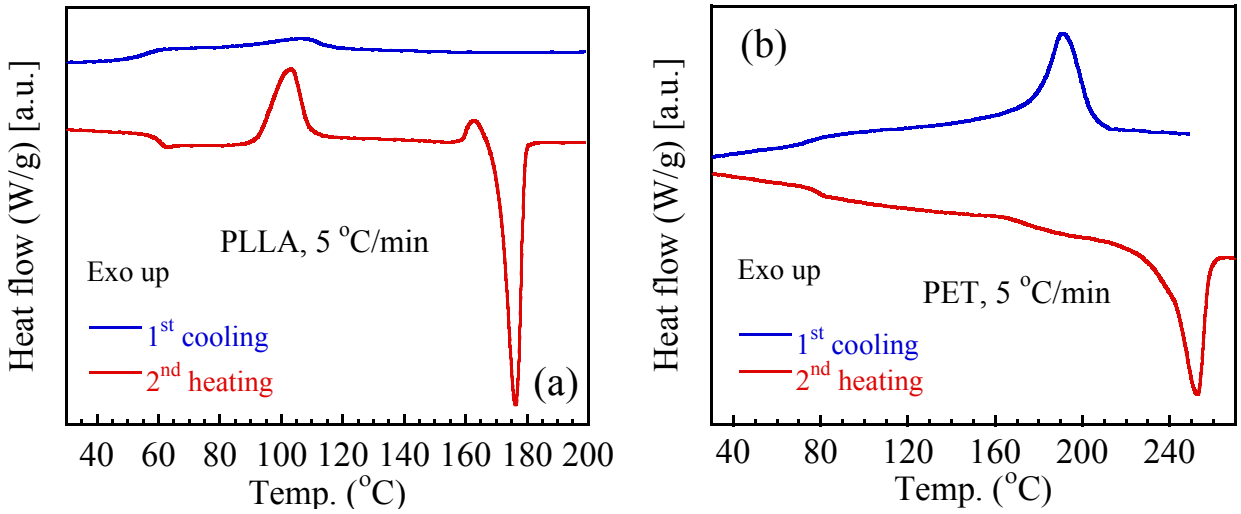

Fig. S.2. DSC thermograms of (a) PLLA and (b) PET. Heating and cooling rates were set equal to 5 °C/min.

D.2. Additional data on PET:

Fig. S.3. represents the *ex situ* WAXD and SAXS data of nano-confined-crystalline PET (ncc-PET), resulting from annealing of the pre-melt-stretched PET. Similar to the case of ncc-PLLA, the oriented crystallization can be inferred from the 2D WAXD pattern. From the SAXS intensity profile along scattering maxima direction as showed of the image inserted in Fig. S.3b, the long period L_p of ncc-PET can be estimated equal to $2\pi/q_{max}$ = 7.5 nm. This value is lower than the reported value of 8 to 14 nm for the isotopic semi-crystalline PET in the literature [9]. The large difference in L_p of ncc-PLLA (15 nm) and ncc-PET (7.5 nm) reflects a difference in the mesh size of the chain network.

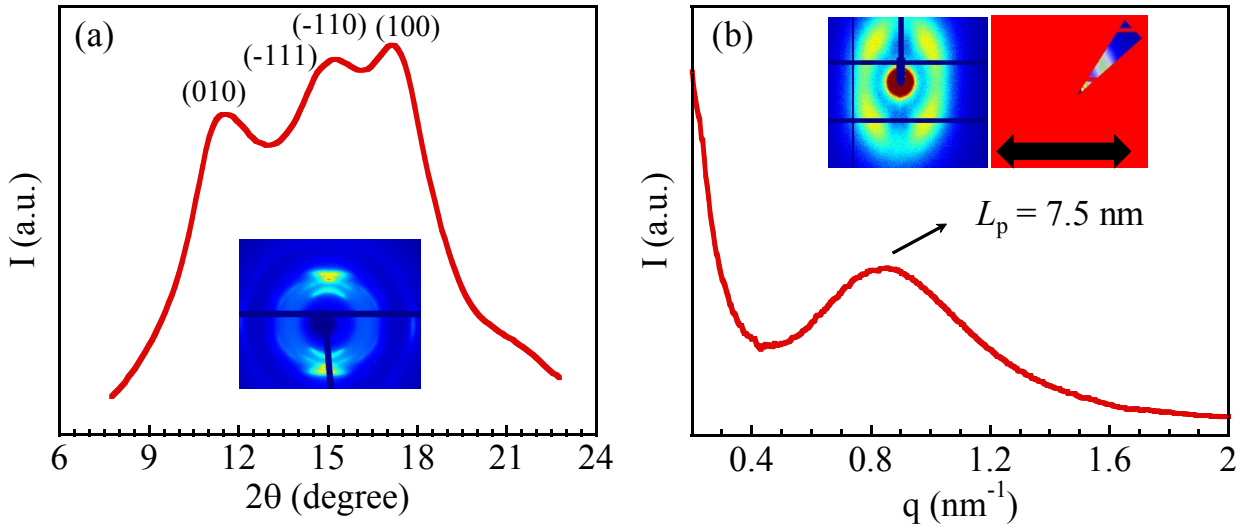

Fig. S.3. X-ray scattering intensity profiles along with corresponding 2D patterns as inset images of nano-confined-crystalline PET: (a) WAXD data and (b) SAXS data. Stretching direction is horizontal.

To acquire more detailed information regarding the cold crystallization of pre-melt-stretched PET, *in situ* WAXD and SAXS measurements were also carried out during annealing of the sample at 100 ˚C. Figs. S.4(a-b) present the 2D WAXD and SAXS patterns along with crystallinity development and long-period evolution over the time span of 1400 s.

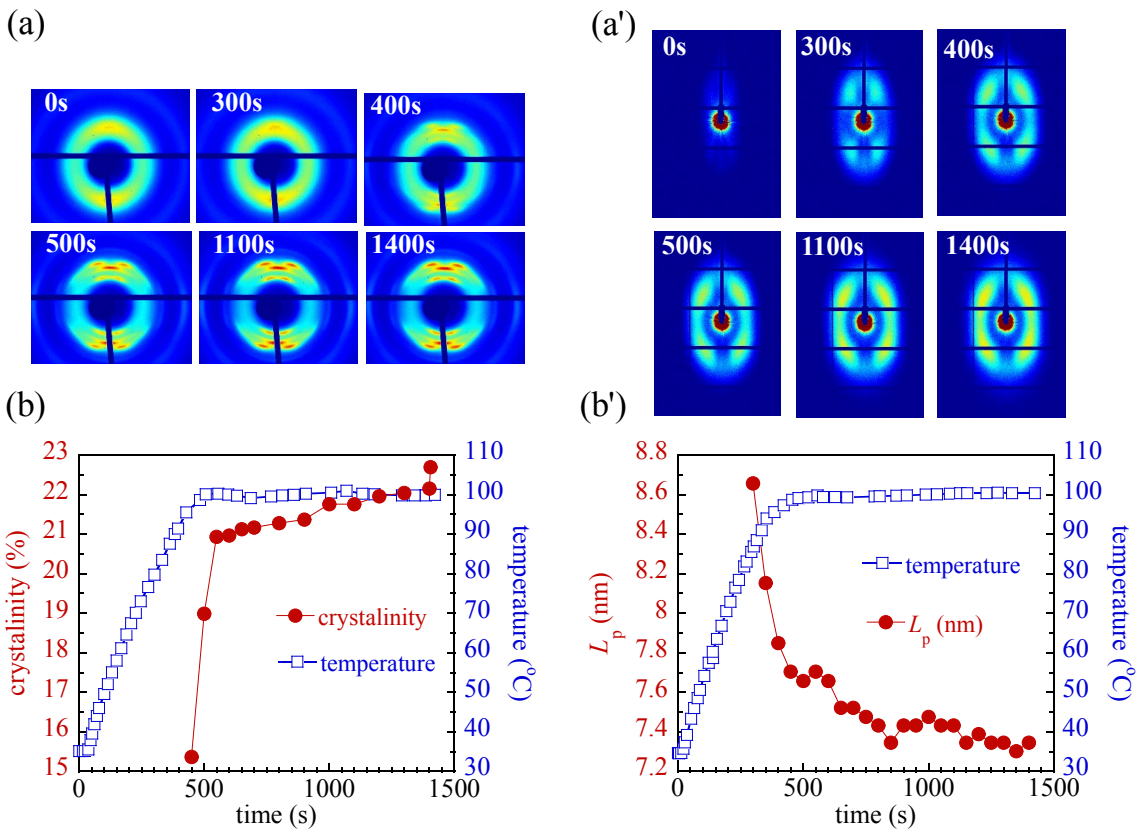

Fig. S.4. *In situ* x-ray scattering measurements during annealing of pre-melt-stretched PET in terms of (a) 2D WAXD pattern, (a') 2D SAXS pattern, (b) crystallinity increase, (b') evolution of the long period L_p, where the temperature rise as a function of time is given in terms of the squares.

Mechanical properties in terms of uniaxial tensile deformation of ncc-PET at room temperature is shown in Fig. S.5 in comparison to the isotropic semi-crystalline PET. The characteristic is similar to that presented in Fig. 6 for ncc-PLLA.

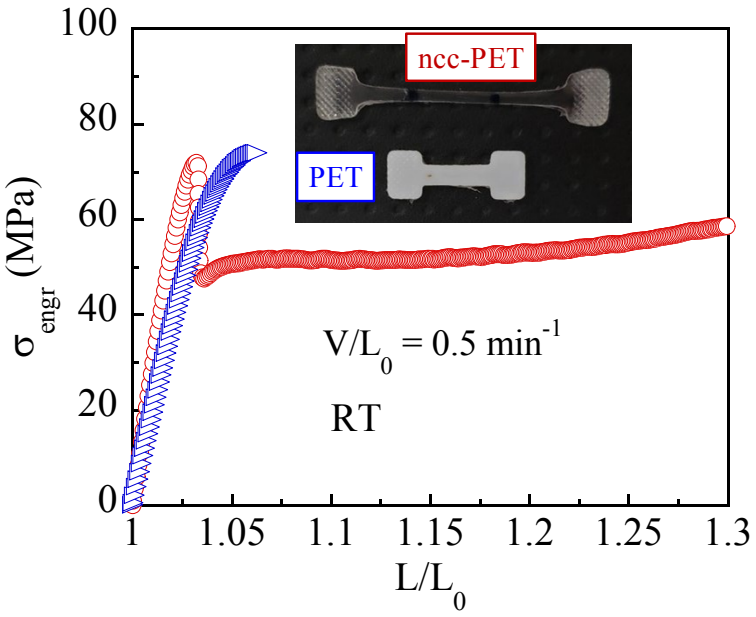

Fig. S.5. Engineering stress σ_{engr} vs draw ratio L/L_0 from uniaxial tensile test of crystalline PET and ncc-PET at room temperature (RT). The inset image contrasts the appearance of two types of semi-crystalline PET; opaque semi-crystalline PET vs. transparent nano-confined-crystalline PET.

References:

[1] M. Razavi, S.-Q. Wang, *Macromolecules* **2019**, *52*, 5429.
[2] I. Stolte, R. Androsch, M. L. Di Lorenzo, C. Schick, *The Journal of Physical Chemistry B* **2013**, *117*, 15196.
[3] S. Cheng, S.-Q. Wang, *Macromolecules* **2014**, *47*, 3661.
[4] S.-Q. Wang, "*Nonlinear Polymer Rheology: Macroscopic phenomenology and Molecular foundation*", Wiley, Hoboken, NJ, 2018.
[5] S.-Q. Wang, S. Cheng, P. Lin, X. Li, *The Journal of chemical physics* **2014**, *141*, 094905.
[6] D. H. Ender, R. D. Andrews, *J. Appl. Phys.* **1965**, *36*, 3057.
[7] G. D. Zartman, S. Cheng, X. Li, F. Lin, M. L. Becker, S.-Q. Wang, *Macromolecules* **2012**, *45*, 6719.
[8] M. Razavi, S.-Q. Wang, *Macromolecules* **2019**, *52*, 5429.
[9] L. A. Baldenegro-Perez, D. Navarro-Rodriguez, F. J. Medellin-Rodriguez, B. Hsiao, C. A. Avila-Orta, I. Sics, *Polymers* **2014**, *6*, 583.